A comparison of latent heat fluxes over global oceans for ERA and NCEP with GSSTF2

Licheng Feng[1,2] and Jianping Li[1,2]

Received 30 September 2005; revised 13 December 2005; accepted 16 December 2005; published 9 February 2006.

[1] The ECMWF Re-Analysis (ERA) and NCEP reanalysis monthly latent heat flux (LHF) data are compared with those of the Goddard Satellite-Based Surface Turbulent Fluxes, version2 (GSSTF2), respectively, during the period of 1988–2000, over the global oceans between 60°S and 60°N. Qualitatively, the annual mean LHF fields and monthly variations are similar for GSSTF2, ERA, and NCEP. Quantitatively, however, there are distinct differences among them. The annual mean ERA LHF is closer to GSSTF2 than NCEP in the tropics (5°–25°S and 8°–22°N) and midlatitudes, while the situation is opposite in other zones. The temporal variability of monthly LHF difference (ERA-GSSTF2) is smaller than that of NCEP-GSSTF2 in the tropics, yet the former and the latter are similar in other zones. To find causes for the discrepancies of LHF, the differences of both the 10-m wind speed (U_{10m}) and sea-air humidity difference ($Q_{s\text{-}a}$) among these data sets have been studied. The differences of the annual mean fields and the monthly variations of the differences between GSSTF2 and the other two data sets in the tropics may be mainly caused by the discrepancies of both U_{10m} and $Q_{s\text{-}a}$.
Citation: Feng, L., and J. Li (2006), A comparison of latent heat fluxes over global oceans for ERA and NCEP with GSSTF2, *Geophys. Res. Lett.*, *33*, L03810, doi:10.1029/2005GL024677.

1. Introduction

[2] The exchange of energy and material across the air-sea interface mainly include heat, momentum and freshwater. These fluxes are generally used to study air-sea interactions and are required for driving ocean models, and evaluating numerical weather prediction (NWP). In these fluxes, the variability of surface heat flux is dominated by the latent heat flux (LHF) due to its large amplitude of interannual and spatial variability [*da Silva et al.*, 1994; *Kubota et al.*, 2003]. Therefore, it is important to obtain high quality LHF data over global oceans. The LHF data sets can be roughly divided into three categories, that is, the observation data sets, for example, the Comprehensive Ocean-Atmosphere Data Set (COADS) [*Woodruff et al.*, 1993], the NWP products, such as the ECMWF Re-Analysis (ERA), the National Centers for Environmental Predication reanalysis 1 (NCEP) [*Kalnay et al.*, 1996] and reanalysis 2 (NCEP2) [*Kanamitsu et al.*, 2002], and those constructed from satellite data, for instance the Goddard Satellite-Based Surface Turbulent Fluxes, version2 (GSSTF2) [*Chou et al.*, 2004]. In these data sets the COADS, ERA, and NCEP are widely used. Since the COADS-based fluxes have serious sampling problems [*da Silva et al.*, 1994], this study focuses on evaluating the ERA and NCEP data, which can provide longtime (several decades) global LHF data. The aim is to find advantages and limitations of each data, and provide useful guidance for improving atmospheric General Circulation Models (GCMs). Further study attempts to find the sources of errors in each data. There is no sea truth for monthly gridded LHF products, but based on comparison with high-quality flux observations, the GSSTF2 LHF, surface air humidity, and winds are likely to be accurate [*Brunke et al.*, 2002, 2003; *Chou et al.*, 2004]. Thus we compare the ERA and NCEP with GSSTF2. *Chou et al.* [2004] compared the NCEP with GSSTF2 for 1992–93. In this study we will take the ERA into consideration, and extend the period to 13 years (1988–2000). The ERA (with 2.5° resolution) and NCEP (Gaussian grid about 1.8°) data are both interpolated to a regular 1° × 1° grid using bilinear-interpolation to remain consistent with the GSSTF2.

2. Intercomparison

[3] Figure 1 shows the annual mean LHF of GSSTF2, the annual mean LHF differences ERA-GSSTF2 and NCEP-GSSTF2 (1988–2000), respectively, over the global oceans (60°S–60°N). Figure 1a illustrates that the large values (>160 W m^{-2}) are located in the tropics (5°–20°S and 10°–25°N) except the Indian Oceans (10°–30°S). There are also large values in the western boundary current regions of the Kuroshio and Gulf Stream, which are caused by high surface winds (~8–9 m s^{-1}) (not shown) coupled with large sea-air humidity difference ($Q_{s\text{-}a}$) (not shown) in these areas. The small values (<80 W m^{-2}) are found in the equatorial oceans (10°S–10°N) due to weak winds (~4–5 m s^{-1}) (not shown) and low sea surface temperature (SST) caused by the upwelling in the eastern boundary. In the high latitudes the LHF is also small since the temperature is low. The large scale distributions of the annual mean LHF fields are basically accordant for GSSTF2, ERA (not shown) and NCEP (not shown), but there are obvious differences in some regions. Figure 1b reveals that the ERA LHF is larger than GSSTF2 in the equatorial Indian Ocean (10°S–10°N), tropical Pacific (except the central part), equatorial Atlantic, and subtropics (25°–35°), with the largest difference exceeding 40 W m^{-2}. The case is opposite for the rest, especially in the eastern South Pacific, with the largest difference beyond 40 W m^{-2}. Figure 1c suggests that in the eastern South Pacific, the region of the discrepancies

[1] State Key Laboratory of Numerical Modeling for Atmospheric Sciences and Geophysical Fluid Dynamics (LASG), Institute of Atmospheric Physics, Chinese Academy of Sciences, Beijing, China.
[2] Also at Graduate School of the Chinese Academy of Sciences, Beijing, China.

0094-8276/06/2005GL024677$05.00

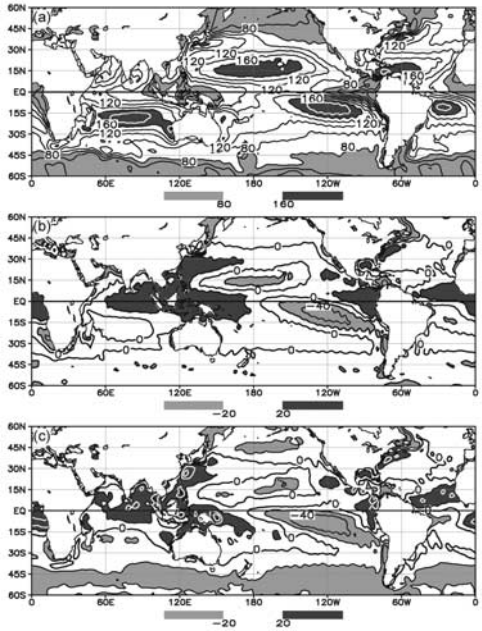

Figure 1. (a) The annual mean LHF from GSSTF2. (b) The annual mean LHF difference ERA-GSSTF2. (c) Same as in Figure 1b, but for NCEP-GSSTF2. The period is 1988–2000. The contour interval is 20 W m^{-2}. Units in W m^{-2}.

NCEP-GSSTF2 exceeding 40 W m^{-2} is larger than that of ERA-GSSTF2, but the maximum difference is obviously smaller than the 2-yr result (~60 W m^{-2}) of *Chou et al.* [2004]. In the 40°–60° latitudes of both hemispheres, especially in the SH, the differences are also significantly larger than those of ERA-GSSTF2, and in the Northern Hemisphere (NH) the discrepancies are larger than the result of *Chou et al.* [2004].

[4] To further study the meridional characteristics of LHF and the differences among the three data sets, we displayed the zonal-mean LHF profiles in Figure 2. Figure 2a shows that the LHF reaches maximum at approximately 15° in both hemispheres. The LHF also decreases equatorward and poleward reaches a minimum in the equator and in high latitudes. In Figure 2b the zonal-mean LHF reveals that in the oceans south of 18°S, the ERA LHF is closer to GSSTF2 than NCEP, in the tropics (18°S–8°N), the situation is opposite, and in the oceans north of 35°N, the ERA and NCEP LHF are similar. Since the zonal averages of the LHF differences only show the mean zonal errors, we calculated the zonal means of the absolute LHF differences of ERA-GSSTF2 and NCEP-GSSTF2 to investigate the amplitude of deviations between GSSTF2 and the other two data sets. It suggests that in the tropics (5°–25°S and 8°–22°N) and midlatitudes (35°–60°), the zonal means of the absolute LHF value of ERA-GSSTF2 is smaller than that of NCEP-GSSTF2, while in the equatorial band (3°S–8°N) and the subtropics the situation is reverse. It's not completely consistent with the zonal-mean LHF in the tropics and subtropics of the SH, indicating that in those areas the large positive and negative errors between NCEP and GSSTF2 along the latitude circle are canceled, and small zonal average errors are obtained. In conclusion, the annual mean LHF of ERA is closer to GSSTF2 than NCEP

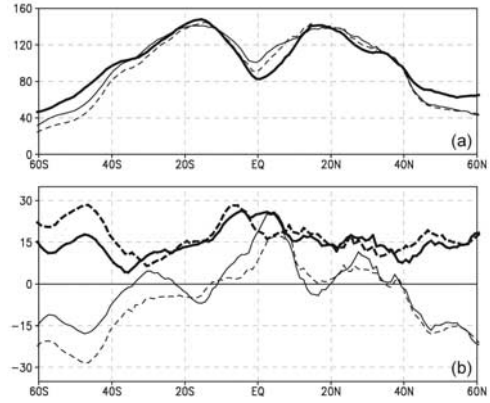

Figure 2. Meridional profiles of the zonal average for (a) the annual mean LHF from GSSTF2 (bold solid line), ERA (thin solid line) and NCEP (dashed line), (b) the differences in annual mean LHF ERA-GSSTF2 (thin solid line) and NCEP-GSSTF2 (thin dashed line), and the absolute differences in annual mean LHF ERA-GSSTF2 (bold solid line) and NCEP-GSSTF2 (bold dashed line). Units in W m^{-2}.

in the midlatitudes and tropics but the case is opposite in the equatorial band and the subtropics.

[5] When comparing two data sets it's necessary to know the standard deviations of differences (SDD) [*Chou et al.*, 2004] and temporal cross-correlation coefficients (CCC) between them, which are used to measure the consistency of the temporal variability of the two. Figure 3 shows the SDD and CCC of monthly LHF between GSSTF2 and the other two products. Figure 3a reveals that the SDD in LHF has large values (~25–35 W m^{-2}) in the tropics, however, in the equatorial Indian Ocean, eastern and western parts of the equatorial Pacific and equatorial Atlantic the values are relatively small (<15 W m^{-2}). In the extratropics the SDD in LHF is also small. The CCC between GSSTF2 and ERA (Figure 3b) has low values (0.6–0.8) in the tropics, especially in the equatorial oceans where it has a minimum (~0.6), and increases poleward. The results above suggest

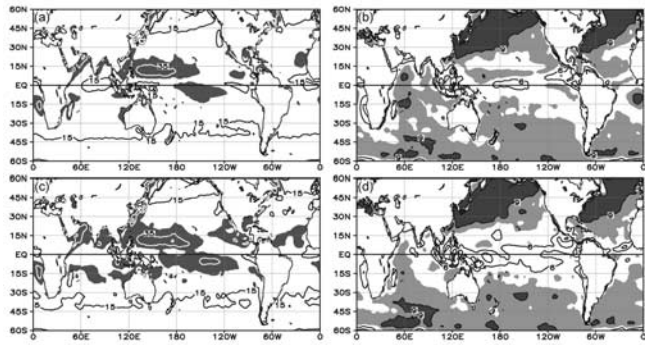

Figure 3. (a) The SDD of monthly LHF between GSSTF2 and ERA (in W m^{-2}). (b) The CCC (multiplied by 10) of monthly LHF between GSSTF2 and ERA. (c) Same as in Figure 3a, but for NCEP. (d) Same as in Figure 3b, but for NCEP. The SDD in excess of 25 W m^{-2} is shaded dark. The CCC (multiplied by 10) excess of 8 (9) is shaded light (dark).

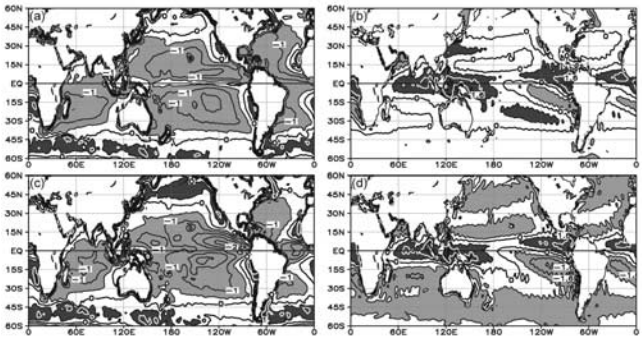

Figure 4. (a) The annual mean U_{10m} (in m s^{-1}) difference ERA-GSSTF2. (b) The annual mean $Q_{s\text{-}a}$ (in g kg^{-1}) difference ERA-GSSTF2. (c) Same as in Figure 4a, but for NCEP. (d) Same as in Figure 4b, but for NCEP. The U_{10m} and $Q_{s\text{-}a}$ differences greater (smaller) than 0.5 m s^{-1} and 0.8 g kg^{-1} (−0.5 and −0.8) are shaded dark (light), respectively.

that the monthly LHF (ERA-GSSTF2) has great temporal variability in the tropics. Figures 3c and 3d roughly imply the same patterns as Figures 3a and 3b, however, there are some significant differences. In the tropics, the regions of the SDD in LHF (NCEP-GSSTF2) beyond 25 W m^{-2} are larger than LHF (ERA-GSSTF2). The CCC between the monthly NCEP and GSSTF2 LHF in the area stated above is obviously lower than that between ERA and GSSTF2. Thus the variability of monthly LHF (ERA-GSSTF2) is smaller than that of NCEP-GSSTF2 in the tropics.

3. Influence of Wind and $Q_{s\text{-}a}$

[6] There are mainly two sources of errors for LHF, one is from the warps of the bulk variables, the other is from the way of considering salinity effect, turbulent exchange coefficients and so on in the algorithm [*Brunke et al.*, 2002]. In this paper we will focus on the comparison of bulk variables.

[7] In Figure 4, the annual mean U10m and Qs-a differences between ERA, NCEP and GSSTF2 are displayed, respectively. Figure 4a implies that the ERA U10m is smaller than GSSTF2 in the oceans between 40°S and 40°N, and larger than the latter in other zones. Figure 4c is similar to Figure 4a, but they differ in the North Pacific (40°−60°N), where the ERA U10m agrees better with the GSSTF2 than NCEP. The distributions of Figure 4b are similar to Figure 1b in most regions, indicating that in these regions the LHF difference (ERA-GSSTF2) is possibly mainly resulted from the difference in Qs-a. However, in the central part of the North Pacific, the LHF difference (ERA-GSSTF2) is possibly mainly caused by the difference in U10m (Figure 4a). In the central part of the South Pacific negative U10m difference and positive Qs-a difference resulted in small LHF difference. Figure 4d shows that the NCEP $Q_{s\text{-}a}$ is larger than GSSTF2 in the equatorial band, and smaller than the latter in other zones. It compares well with Figure 1c in most regions, which suggests that the LHF difference (NCEP-GSSTF2) maybe mainly resulted from the $Q_{s\text{-}a}$ difference, especially in the North Pacific and the oceans south of 40°S, where the negative $Q_{s\text{-}a}$ difference counteract the positive U_{10m} difference to get negative LHF difference.

[8] To study the temporal variability of the U_{10m} and Q_{s-a} differences between GSSTF2 and the other two data sets, the SDD and CCC are shown in Figures 5 and 6. Figures 5a and 5c indicate that the regions of the SDD in U_{10m} (ERA-GSSTF2) beyond 0.6 m s^{-1} are smaller than U_{10m} (NCEP-GSSTF2) in the tropics and SH. It implies the temporal variability of monthly U_{10m} difference (ERA-GSSTF2) is smaller than NCEP-GSSTF2 in those areas. Figures 5b and 5d show the CCC in U_{10m} between GSSTF2 and ERA, NCEP, respectively. They both have high values in most regions of the global oceans (∼0.8−0.9), which means there is good agreement between GSSTF2 and the other two data sets in the temporal variability of monthly U_{10m}. As to comparing Figures 5b and 5d, it can be said that in the equatorial oceans and SH the CCC in U_{10m} between GSSTF2 and ERA is larger than that between GSSTF2 and NCEP, suggesting that in these areas the monthly variations of the ERA U_{10m} is closer to GSSTF2 than NCEP. Figures 6a and 6c indicate that the regions of the SDD in $Q_{s\text{-}a}$ (ERA-GSSTF2) beyond 0.8 g kg^{-1} are smaller than $Q_{s\text{-}a}$ (NCEP-GSSTF2) in the tropics and subtropics. Figures 6b and 6d show the CCC in $Q_{s\text{-}a}$ between GSSTF2 and ERA, NCEP, respectively. As to comparing Figures 6b and 6d, it can be said that in most regions the CCC in $Q_{s\text{-}a}$ between GSSTF2 and ERA is larger than that between GSSTF2 and NCEP. Comparing Figures 3, 5, and 6, it can

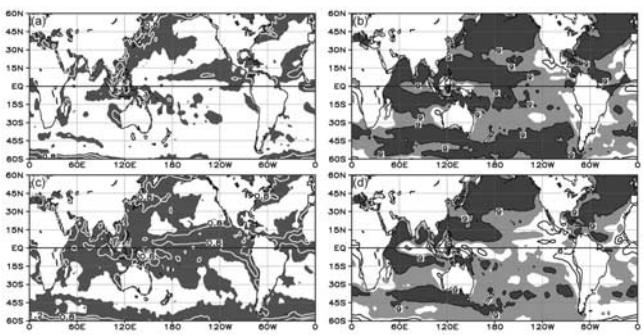

Figure 5. Same as Figure 3 but for U_{10m} (in m s^{-1}). The SDD greater than 0.6 m s^{-1} is shaded dark. The CCC (multiplied by 10) greater than 8 (9) is shaded light (dark).

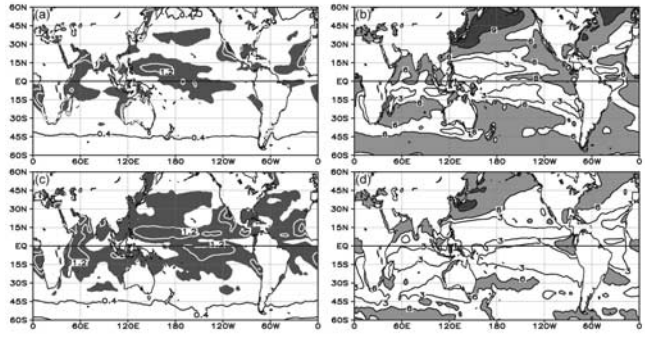

Figure 6. Same as Figure 3 but for $Q_{s\text{-}a}$ (in g kg^{-1}). The SDD greater than 0.8 g kg^{-1} is shaded dark. The CCC (multiplied by 10) greater than 6 (9) is shaded light (dark).

be seen that in the tropics the SDD in LHF (ERA-GSSTF2) is smaller than NCEP-GSSTF2 (Figures 3a and 3c), this can be explained by the smaller SDD in U_{10m} and $Q_{s\text{-}a}$ (ERA-GSSTF2) (Figures 5a, 5c, 6a, and 6c). The CCC (Figures 3b, 3d, 5b, 5d, 6b, and 6d) has the same characters in that area.

4. Conclusions

[9] Two widely used NWP products namely ERA and NCEP are compared with GSSTF2 in LHF and U_{10m}, for 1988–2000, over the global oceans (60°S–60°N). The three products agree well in depicting the general characteristics of the LHF, U_{10m} and $Q_{s\text{-}a}$, but they have distinct differences in some areas. For the annual mean field, the ERA LHF agrees well with GSSTF2 in the tropics (5°–25°S and 8°–22°N) and midlatitudes, and the good agreement maybe a result of the small difference in U_{10m} and $Q_{s\text{-}a}$ between the data sets. The NCEP LHF compares positively with GSSTF2 in the equatorial band and subtropics of both hemispheres. With regards to the monthly variation of the LHF, ERA is closer to GSSTF2 than NCEP in the tropics, which can possibly be explained by the smaller monthly variation in U_{10m} and $Q_{s\text{-}a}$ differences.

[10] **Acknowledgments.** This work was supported jointly by the NSFC Project (40325015), 973-project (2006CB400503), and CAS International Partnership Creative Group (Climate System Model Development and Application Studies). Revision of the manuscript has been assisted by helpful comments from two anonymous reviewers and Ms. Misha Bowles for improving the English of the manuscript.

References

Brunke, M. A., X. Zeng, and S. Anderson (2002), Uncertainties in sea surface turbulent flux algorithms and data sets, *J. Geophys. Res.*, *107*(C10), 3141, doi:10.1029/2001JC000992.

Brunke, M. A., C. W. Fairall, X. Zeng, L. Eymard, and J. A. Curry (2003), Which bulk aerodynamic algorithms are least problematic in computing ocean surface turbulent fluxes?, *J. Clim.*, *16*, 619–635.

Chou, S.-H., E. Nelkin, J. Ardizzone, and R. M. Atlas (2004), A comparison of latent heat fluxes over global oceans for four flux products, *J. Clim.*, *17*, 3973–3989.

da Silva, A., C. C. Young, and S. Levitus (1994), *Algorithms and Procedures,* vol. 1, *Atlas of Surface Marine Data 1994*, *NOAA Atlas NESDIS 6*, 83 pp., Gov. Print. Off., Washington, D. C.

Kalnay, E., et al. (1996), The NCEP/NCAR 40-year reanalysis project, *Bull. Am. Meteorol. Soc.*, *77*, 437–471.

Kanamitsu, M., W. Ebisuzaki, J. Woollen, S.-K. Yang, J. J. Hnilo, M. Fiorino, and G. L. Potter (2002), NCEP-DOE AMIP-II reanalysis (R-2), *Bull. Am. Meteorol. Soc.*, *83*, 1631–1643.

Kubota, M., A. Kano, H. Muramatsu, and H. Tomita (2003), Intercomparison of various surface latent heat flux fields, *J. Clim.*, *16*, 670–678.

Woodruff, S. D., S. J. Lubker, K. Wolter, S. J. Worley, and J. D. Elm (1993), Comprehensive Ocean–Atmosphere Data Set (COADS) release la: 1980–92, *Earth Syst. Monit.*, *4*, 4–8.

L. Feng and J. Li, LASG, Institute of Atmospheric Physics, Chinese Academy of Sciences, Beijing 100029, China. (fenglichg@163.com.cn; ljp@lasg.iap.ac.cn)